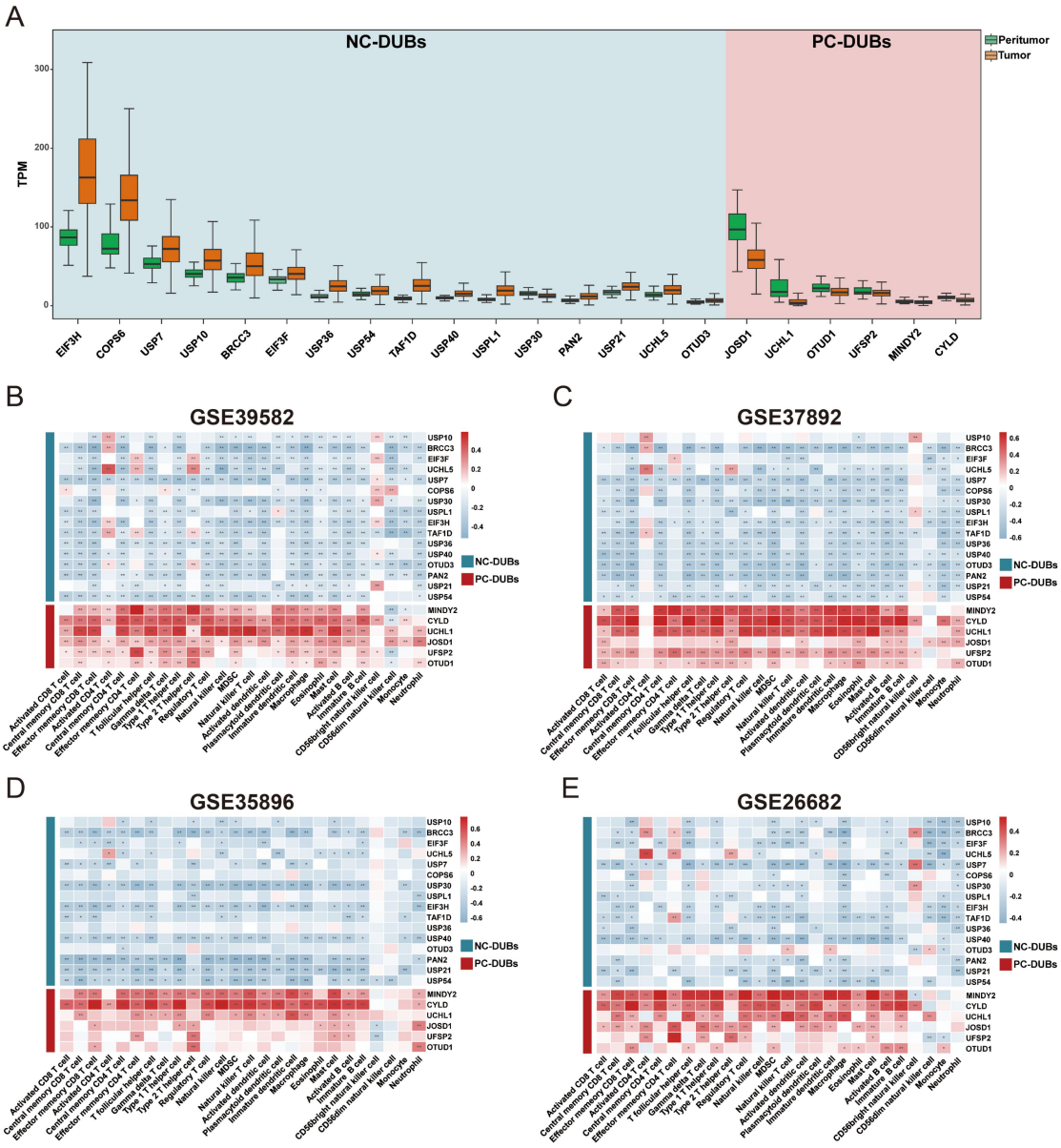

Figure S1. Related to Figure 1. (A). The expression of IR-DUBs in tumors and peritumor tissues in the TCGA cohort. Correlation of IR-DUBs with infiltrated immune cells in MSS CRC in (B) GSE39582, (C) GSE37892, (D) GSE35896, (E) GSE26682.

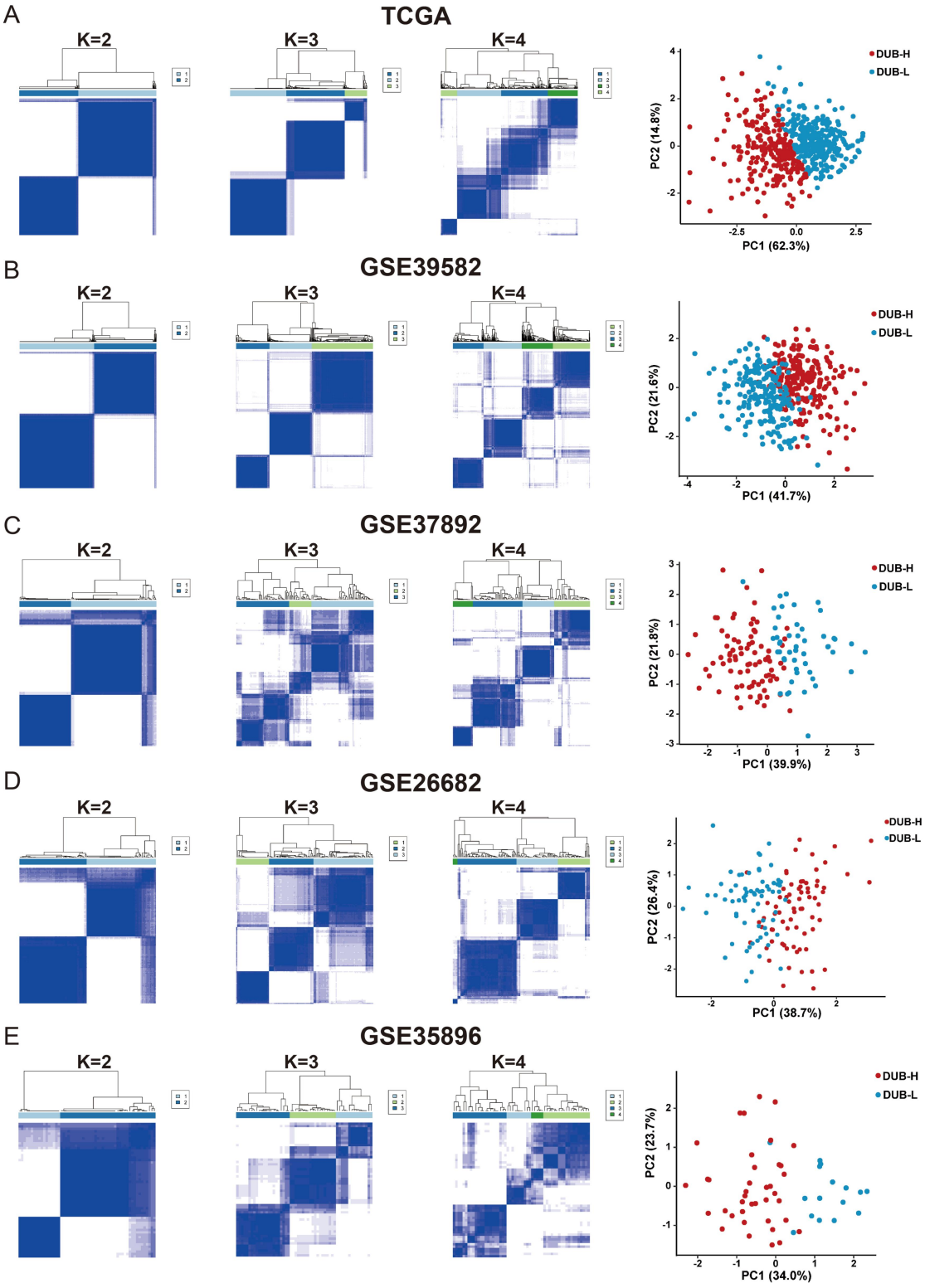

Figure S2. Related to Figure 2. (A-E). Consensus matrices of the TCGA cohort and four GEO cohorts for k = 2 - 4. The PCA results are displayed in the right panel between DUB-L and DUB-H classes

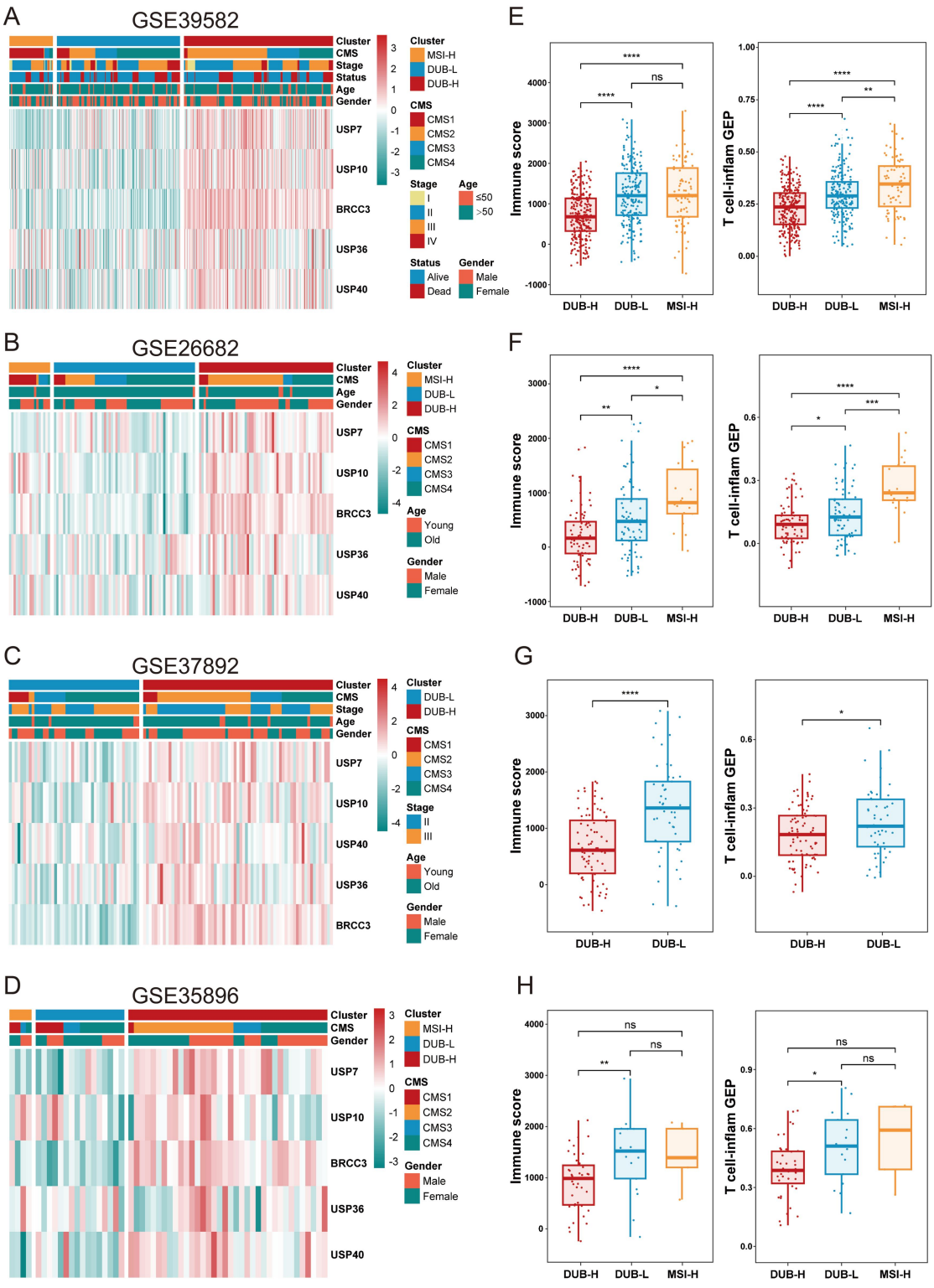
A
GSE39582
Cluster
CMS
Stage
Status
Age
Gender
USP7
USP10
BRCC3
USP36
USP40
Cluster
MSI-H
DUB-L
DUB-H
CMS
CMS1
CMS2
CMS3
CMS4
Stage
I
II
III
IV
Age
≤50
>50
Status
Alive
Dead
Gender
Male
Female
B
GSE26682
Young
Old
C
GSE37892
D
GSE35896
E
F
G
H
Immune score
T cell-inflam GEP
DUB-H
DUB-L
MSI-H
ns

Figure S3. Related to Figure 2. (A-D) Expression spectrum of IR-DUBs within the consensus model and clinical information in DUB-L, DUB-H, and MSI-H CRC samples from (A) GSE39582, (B) GSE26682, (C) GSE37892, and (D) GSE35896 (E-H) Immune score and T cell inflamed GEP in DUB-L, DUB-H, and MSI-H CRC samples from (E) GSE39582, (F) GSE26682, (G) GSE37892, and (H) GSE35896.

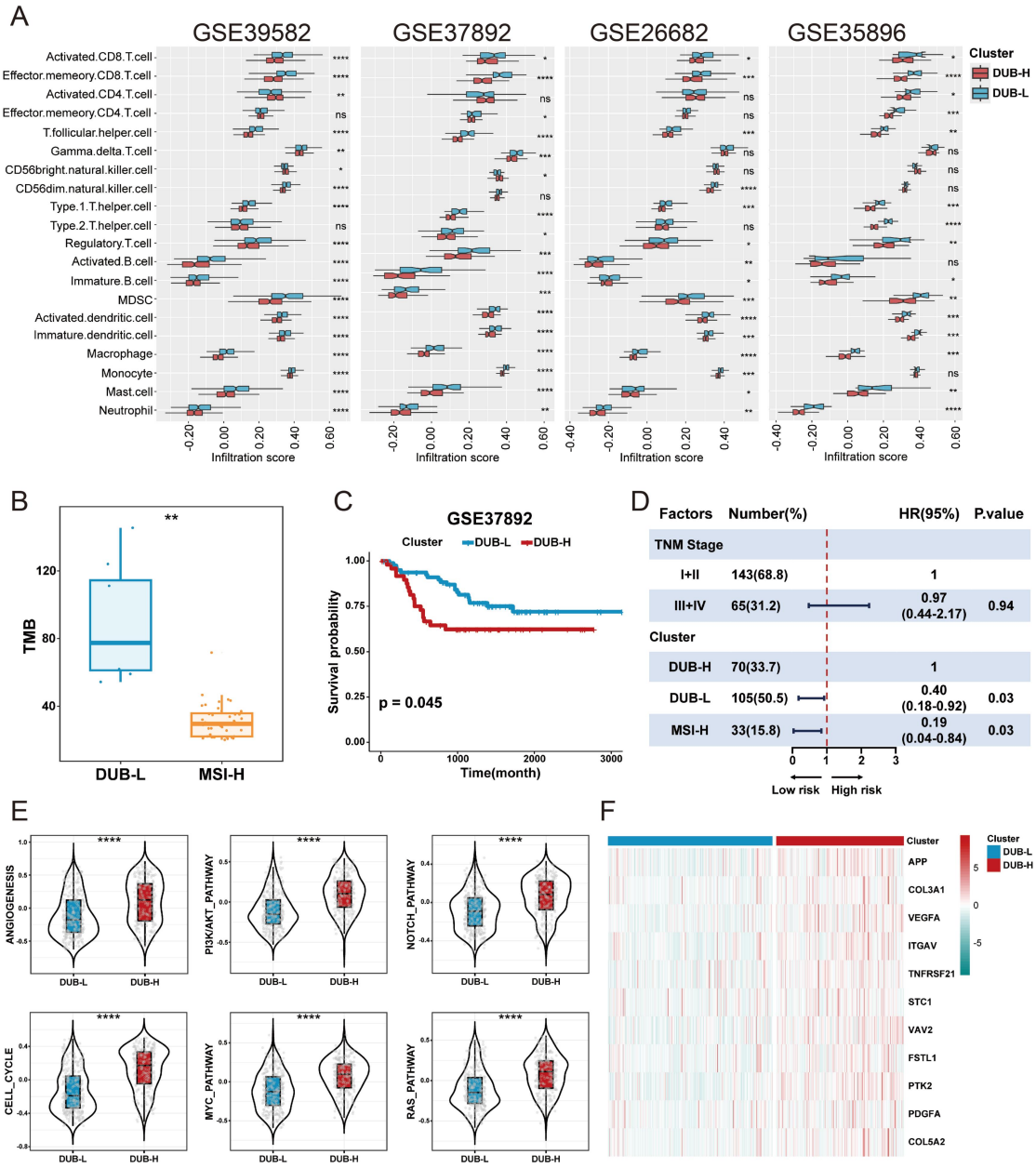

Figure S4. Related to Figure 2. (A). Infiltration score for different types

of immune cells in DUB-L and DUB-H CRC in four GEO cohorts (B). Tumor mutation burden of DUB-L and MSI-H CRC in tumor samples (with a cutoff TMB > 20 mut/Mb) (C). RFS survival plot of DUB-L and DUB-H samples in GSE37892 (D). Multivariate Cox regression of MSS subtypes and TMN stage in the TCGA cohort (E). GSVA enrichment results of DUB-L, DUB-H CRC (F). Heatmap of angiogenesis-related genes in DUB-L, DUB-H CRC

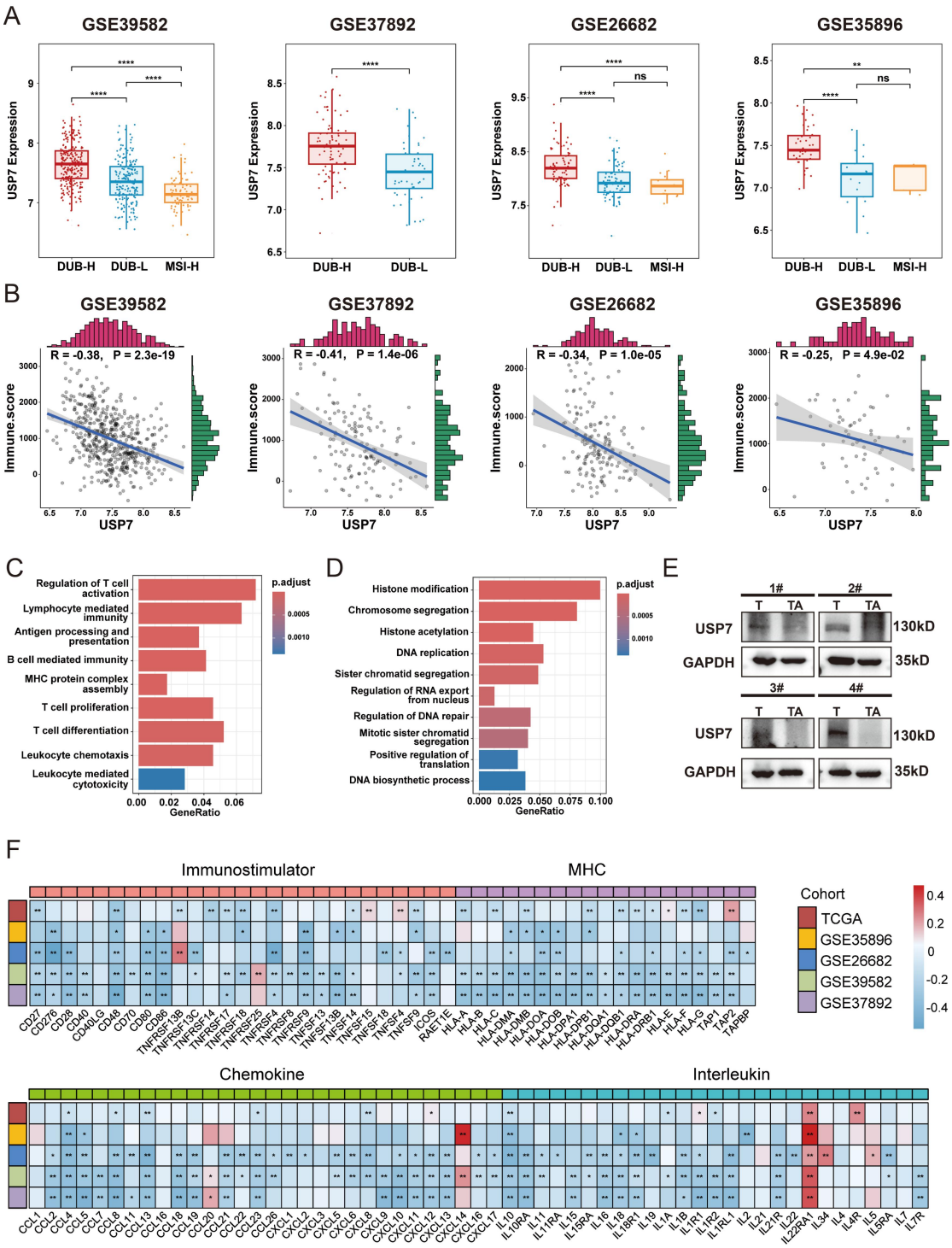
A
GSE39582
GSE37892
GSE26682
GSE35896
USP7 Expression
DUB-H
DUB-L
MSI-H
****
ns
**
B
R = -0.38, P = 2.3e-19
R = -0.41, P = 1.4e-06
R = -0.34, P = 1.0e-05
R = -0.25, P = 4.9e-02
Immune.score
USP7
C
Regulation of T cell activation
Lymphocyte mediated immunity
Antigen processing and presentation
B cell mediated immunity
MHC protein complex assembly
T cell proliferation
T cell differentiation
Leukocyte chemotaxis
Leukocyte mediated cytotoxicity
p.adjust
GeneRatio
D
Histone modification
Chromosome segregation
Histone acetylation
DNA replication
Sister chromatid segregation
Regulation of RNA export from nucleus
Regulation of DNA repair
Mitotic sister chromatid segregation
Positive regulation of translation
DNA biosynthetic process
E
1#
2#
3#
4#
T
TA
USP7
GAPDH
130kD
35kD
F
Immunostimulator
MHC
Chemokine
Interleukin
Cohort
TCGA
GSE35896
GSE26682
GSE39582
GSE37892

Figure S5. Related to Figure 3. (A). USP7 expression in DUB-L, DUB-H and MSI-H tumors in four GEO cohorts. (B). Correlation of USP7 expression with immune score in the MSS CRC samples across four GEO cohorts (C). Signaling pathways enriched in samples with low USP7 expression (D). Signaling pathways enriched in samples with high USP7 expression (E). USP7 protein level in tumor and peritumor tissues (F). Correlation of USP7 expression with immune-related factors in the TCGA and four GEO cohorts.

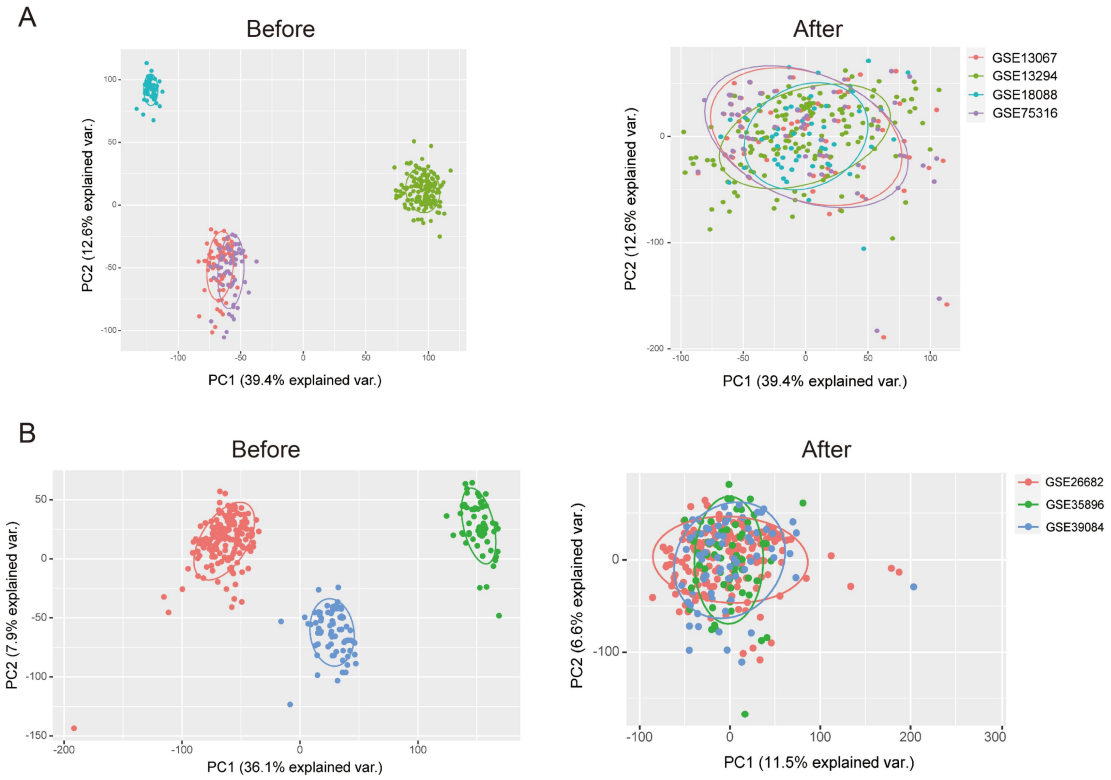

Figure S6. Related to Figure 4. (A-B) PCA analysis demonstrating the batch effects in pooled cohort 1 and cohort 2 before and after combination.

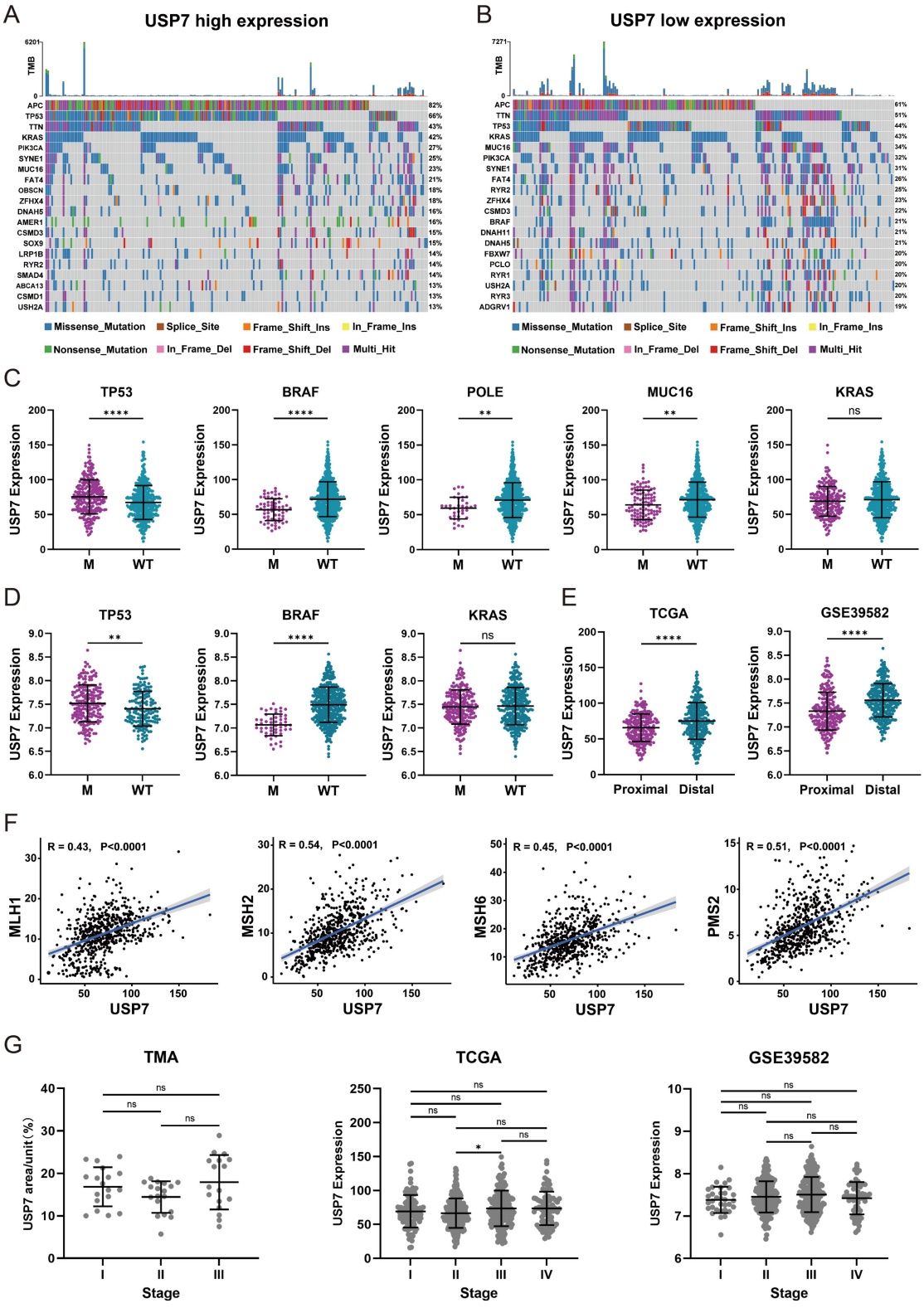

Figure S7. Related to Figure 4. (A). Mutation spectrum of tumorigenesis-related genes in CRC samples with high USP7 expression (B). Mutation spectrum of tumorigenesis-related genes in CRC samples

with low USP7 expression (C). Comparison of USP7 expression between tumorigenesis-related gene mutant and wild-type samples in the TCGA cohort (D). Comparison of USP7 expression between tumorigenesis-related gene mutant and wild-type samples in the GSE39582 cohort. (E). USP7 expression in proximal and distal CRC samples from the TGCA and GSE39582 cohorts (F). Correlation of USP7 expression and four mismatch repair genes (MSH2, MSH6, PMS2, MLH1) (G). USP7 expression across different TNM stages in the local cohort, TCGA and GSE39582 cohort.

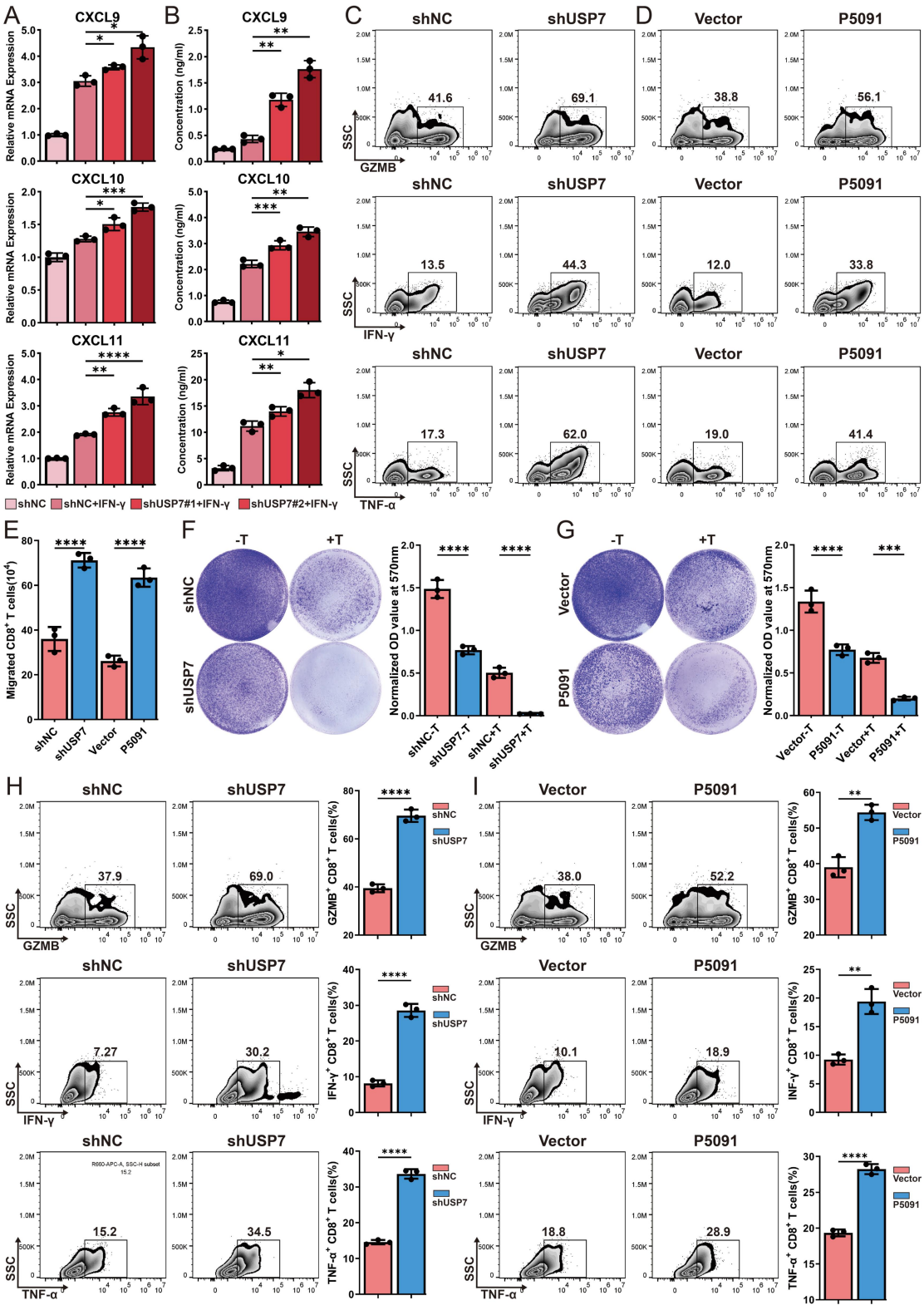
A
CXCL9
CXCL10
CXCL11
Relative mRNA Expression
B
Concentration (ng/ml)
C
shNC
shUSP7
SSC
GZMB
IFN-γ
TNF-α
41.6
69.1
13.5
44.3
17.3
62.0
D
Vector
P5091
38.8
56.1
12.0
33.8
19.0
41.4
shNC
shNC+IFN-γ
shUSP7#1+IFN-γ
shUSP7#2+IFN-γ
E
Migrated CD8+ T cells(10^4)
F
-T
+T
Normalized OD value at 570nm
shNC-T
shUSP7-T
shNC+T
shUSP7+T
G
Vector-T
P5091-T
Vector+T
P5091+T
H
37.9
69.0
7.27
30.2
15.2
34.5
GZMB+ CD8+ T cells(%)
IFN-γ+ CD8+ T cells(%)
TNF-α+ CD8+ T cells(%)
I
38.0
52.2
10.1
18.9
18.8
28.9
INF-γ+ CD8+ T cells(%)

Figure S8. Related to Figure 6. (A). CXCL9, CXCL10 and CXCL11 mRNA expression measured by RT-PCR in the following groups: negative control, negative control + IFN-γ, and USP7 knockdown + IFN-γ in SW1116 cells (B). CXCL9, CXCL10 and CXCL11 protein levels quantified by ELISA in the following groups: negative control, negative control + IFN-γ, and USP7 knockdown + IFN-γ in SW1116 cell supernatants (C). Representative contour plots of $GZMB^+$, $IFN\text{-}\gamma^+$, and $TNF\text{-}\alpha^+$ $CD8^+$ T cells after co-culture with SW480 cells bearing USP7 knockdown or a negative control (D) Representative contour plots of $GZMB^+$, $IFN\text{-}\gamma^+$, and $TNF\text{-}\alpha^+$ $CD8^+$ T cells after co-culture with SW480 cells pretreated with P5091 or a vehicle control (E). Number of migrated CD8+ T cells following their co-culture with SW1116 cells that underwent either USP7 knockdown (vs. negative control) or pharmacological inhibition with P5091 (vs. vehicle control) (F). Representative images and quantitative analysis of T cell-mediated tumor cell-killing in SW1116 cells with USP7 knockdown versus negative control (G). Representative images and quantitative analysis of T cell-mediated killing of SW1116 cells pretreated with P5091 or vehicle control (H). Representative contour plots and proportions of $GZMB^+$, $IFN\text{-}\gamma^+$, and $TNF\text{-}\alpha^+$ $CD8^+$ T cells after co-culture with USP7-knockdown or negative control SW1116 cells (I). Representative contour plots and proportions of $GZMB^+$, $IFN\text{-}\gamma^+$, and $TNF\text{-}\alpha^+$ $CD8^+$ T cells after co-culture with SW1116 cells following P5091 or vehicle control pretreatment.

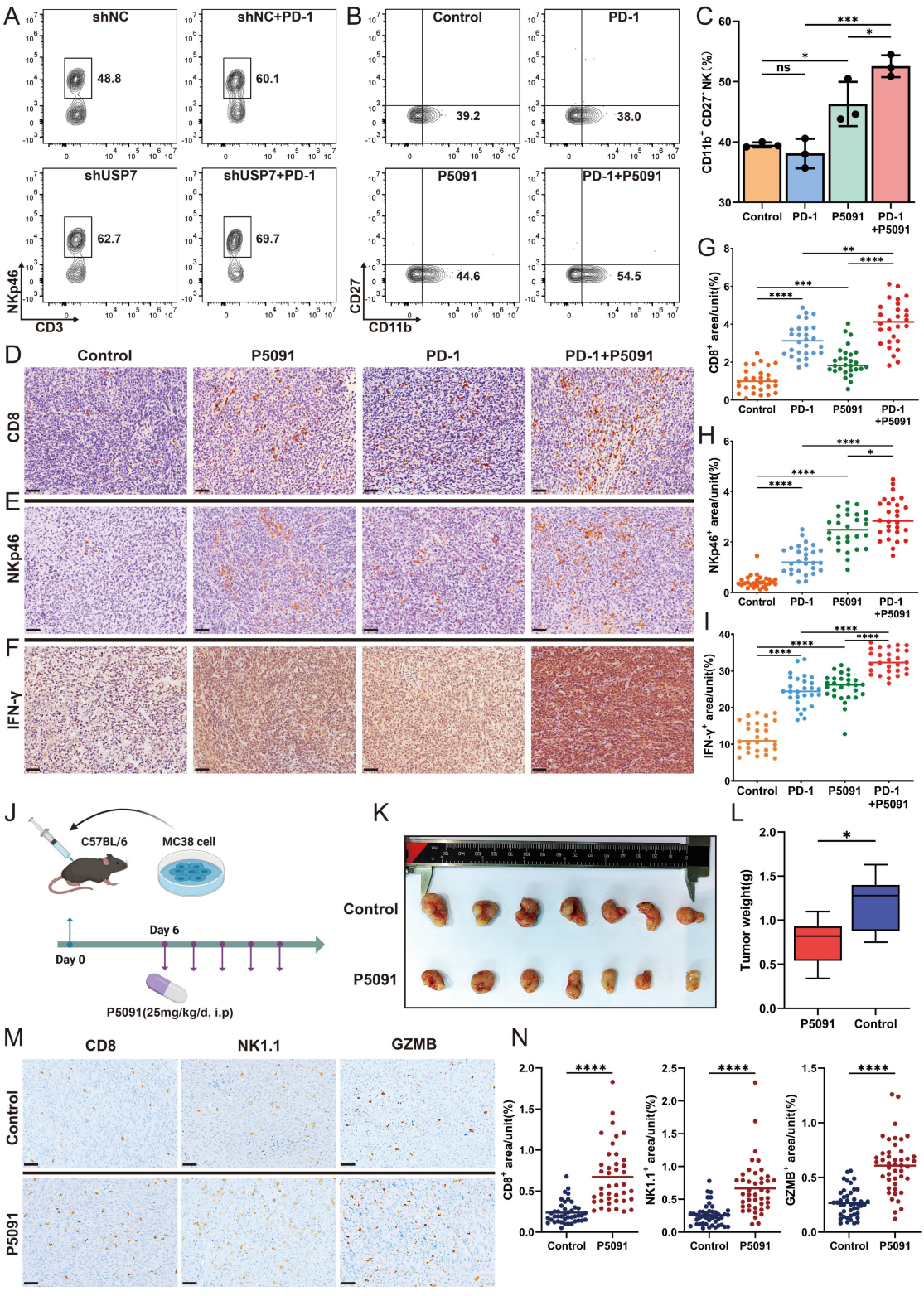
A
shNC
48.8
shNC+PD-1
60.1
shUSP7
62.7
shUSP7+PD-1
69.7
NKp46
CD3
B
Control
39.2
PD-1
38.0
P5091
44.6
PD-1+P5091
54.5
CD27
CD11b
C
CD11b+ CD27- NK (%)
ns
*
***
Control
PD-1
P5091
PD-1 +P5091
D
Control
P5091
PD-1
PD-1+P5091
CD8
E
NKp46
F
IFN-γ
G
CD8+ area/unit(%)
**
****
H
NKp46+ area/unit(%)
I
IFN-γ+ area/unit(%)
J
C57BL/6
MC38 cell
Day 0
Day 6
P5091(25mg/kg/d, i.p)
K
Control
P5091
L
Tumor weight(g)
M
CD8
NK1.1
GZMB
Control
P5091
N
CD8+ area/unit(%)
NK1.1+ area/unit(%)
GZMB+ area/unit(%)

Figure S9. Related to Figure 7&8. (A). Representative contour plots of $CD3^{-}NKp46^{+}$ NK cells in tumors across different groups. (B). Representative contour plots of $CD27^{-}CD11b^{+}$ NK cells in tumors across different groups. (C). Proportions of $CD27^{-}CD11b^{+}$ NK cells in tumors across different groups. (D-F) Representative IHC images of (D) CD8, (E) NKp46 and (F) IFN-γ in tumors from different groups. (G-I) Statistic analysis of (G) CD8, (H) NKp46 and (I) IFN-γ expression in tumors from different groups. (J). Schematic diagram of animal study. C57BL/6 mice was subcutaneously injected with MC38 cells, drug injection (P5091, 25mg/kg/d, i.p.) began on day 6, and tumors were harvested on day 21 (K). Tumor images and between P5091-treated and control groups (L). Tumor weights in P5091-treated and control groups. (M). Representative IHC staining for CD8, NK1.1 and GZMB in P5091-treated and control tumors. (N). Quantification of IHC staining for CD8, NK1.1 and GZMB in P5091-treated and control tumors.

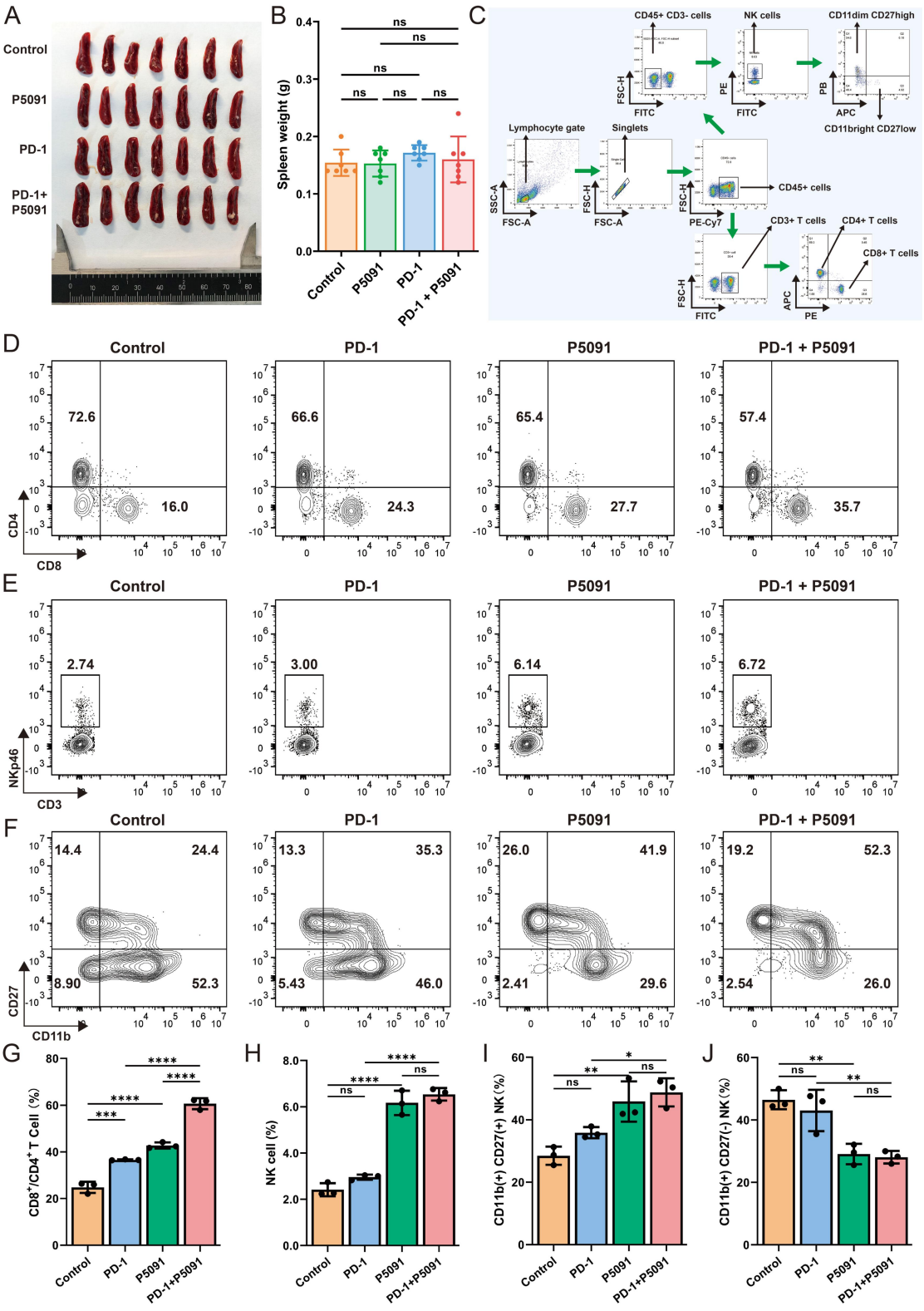

Figure S10. Related to Figure 8. Spleen images (A) and weights (B) of different groups after CT26 mice sacrifice (C) Flow cytometry gating strategy for identifying immune cell populations in tumor tissue: $CD4^+$ T

cells ($CD3^+CD4^+$), $CD8^+$ T cells ($CD3^+CD8^+$), NK cells ($CD3^-NKp46^+$), and $CD11b^+CD27^-$ NK cells. Lymphocytes were gated based on SSC-A vs. FSC-A, and singlets were selected using FSC-A vs. FSC-H (D). Representative flow plots of $CD8^+$ and $CD4^+$ T cells in spleens across different groups (E). Representative flow plots of NK cells in spleens across different groups (F). Representative flow plots of NK cell subtypes in spleens across different groups (G). Ratios of $CD8^+$ to $CD4^+$ T cells in spleens across different groups (H). Proportions of NK cells of spleens in different groups (I). Proportions of $CD11b^+CD27^+$ NK cells across different groups (J). Proportions of $CD11b^+CD27^-$ NK cells across different groups.

Table S1. Correlations of IR-DUBs with infiltrated $CD8^+$T / NK cells in the TCGA cohort

	ssGSEA	MCP-counter	TIMER	CIBERSORT	EPIC	xCell	TIP	quanTIseq
USP10	-	-	-	-	-	-	-	○
USP7	-	○	-	-	-	-	-	○
BRCC3	-	○	-	-	-	-	-	○
EIF3F	-	-	-	○	○	-	-	-
UCHL5	-	-	○	○	-	-	-	○
USP54	-	○	-	-	-	○	-	○
COPS6	-	-	-	○	○	-	○	-
USP30	-	-	○	-	-	-	○	○
USPL1	-	○	○	-	-	-	-	○
EIF3H	-	-	○	○	-	-	○	○
TAF1D	-	-	○	○	-	-	○	○
USP36	-	-	○	○	-	-	○	○
USP40	-	-	○	○	-	-	○	○
OTUD3	-	○	-	○	-	○	○	○
PAN2	-	-	○	○	-	○	○	○
USP21	-	○	○	○	○	-	-	○
MINDY2	+	+	+	+	+	+	+	+
CYLD	+	+	+	+	+	+	+	+
UCHL1	+	+	+	○	+	+	+	+
JOSD1	+	+	+	○	○	+	○	+
UFSP2	+	○	+	○	○	+	○	+
OTUD1	+	○	+	○	○	+	○	+

“+”: positive correlation, **“-”**: negative correlation, **“○”**: Not significant

Table S2. Correlations of NC-DUBs

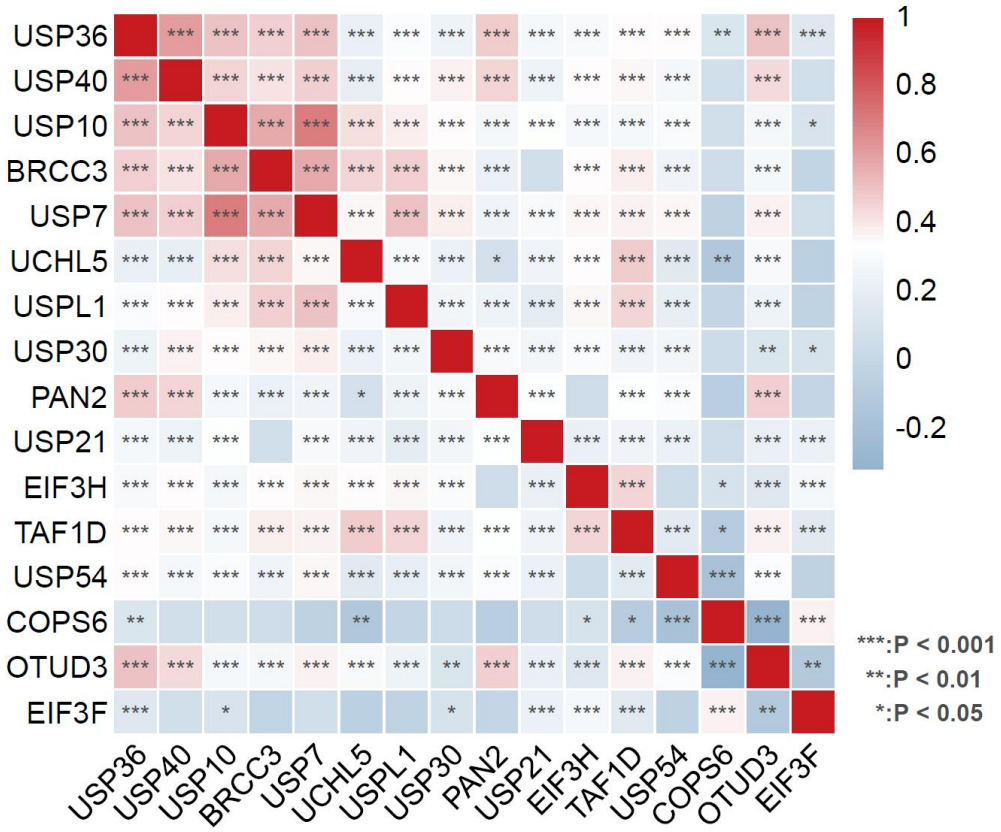

Table S3. Online clinical cohorts used in this study

Cohort	Sample description	platform
TCGA-COAD&READ	529 MSS CRC samples 90 MSI CRC samples	Illumina HiSeq 2000
GSE39582	444 MSS CRC samples 75 MSI CRC samples	GPL570
GSE37892	130 MSS CRC samples	GPL570
Pooled_cohort 1 (GSE13067+GSE13294+ GSE18088+GSE75316)	222 MSS CRC samples 119 MSI CRC samples	GPL570
Pooled_cohort 2 (GSE26682+GSE35896+GSE39084)	252 MSS CRC samples 39 MSI CRC samples	GPL570

Table S4. Clinical features of CRC patients in the Local cohort 1(LC1)

Features			n(%)	
Gender				
	Male		43	(57)
	Female		33	(43)
Age				
	≤60		36	(47)
	>60		40	(53)
TNM Stage				
	I-II		39	(51)
	III-IV		37	(49)
MSI status				
	MSI-H		9	(12)
	MSS		67	(88)
Location				
	Distal		34	(45)
	Proximal		42	(55)

Table S5. Clinical features of CRC patients in the Local cohort 2(LC2)

Features			n(%)	
Gender				
	Male		36	(68)
	Female		17	(32)
Age				
	≤60		21	(40)
	>60		32	(60)
TNM Stage				
	I		18	(34)
	II		18	(34)
	III		17	(32)
MSI status				
	MSI-H		7	(13)
	MSS		46	(87)
Location				
	Distal		26	(49)
	Proximal		27	(51)

Table S6. Clinical features of CRC patients with anti-PD-1 treatment

ID	Gender	Age	Stage	MSI status	Treatment	Response	OS	Status

Patient 1	Female	65	IV	MSS	anti-PD-1	PR	103.5395	Dead
Patient 2	Male	71	IV	MSS	anti-PD-1	PR	426.5968	Dead
Patient 3	Male	66	IV	MSS	anti-PD-1	PR	1099.638	Dead
Patient 4	Male	62	IV	MSS	anti-PD-1	PR	770.5662	Dead
Patient 5	Female	66	IV	MSS	anti-PD-1	PR	677.5172	Dead
Patient 6	Male	59	IV	MSS	anti-PD-1	SD	245.6667	Dead
Patient 7	Female	75	IV	MSS	anti-PD-1	PD	80.50017	Dead
Patient 8	Male	71	IV	MSS	anti-PD-1	SD	328.5172	Dead
Patient 9	Male	57	IV	MSS	anti-PD-1	PD	14.50624	Dead
Patient 10	Male	66	IV	MSS	anti-PD-1	PD	154.5888	Dead

Table S7. Sequences of primers for qRT-PCR.

Gene		Sequence
Human GAPDH	5’Primer	GAGAAGGCTGGGGCTCATTT
	3’Primer	AGTGATGGCATGGACTGTGG
Human USP7	5’Primer	CCCTCCGTGTTTTGTGCGA
	3’Primer	AGACCATGACGTGGAATCAGA
Human CXCL9	5’Primer	TGAGAAAGGGTCGCTGTTCC
	3’Primer	GGGCTTGGGGCAAATTGTTT
Human CXCL10	5’Primer	ACTGCCATTCTGATTTGCTGC
	3’Primer	ATGCAGGTACAGCGTACAGT
Human CXCL11	5’Primer	GAGTGTGAAGGGCATGGCTA
	3’Primer	ATAAGCCTTGCTTGCTTCGAT